energies

MDPI

Article

Coordinated Reactive Power Control with a Variable Shunt Reactor and an Inverter-Based Wind Power Plant

Seung-Ho Song [1,*] and Soo-Bin Kim [2]

[1] Department of Electrical Engineering, Kwangwoon University, Seoul 01897, Korea
[2] Korea Electric Power Research Institute, Daejeon 34056, Korea; ksubi11@kw.ac.kr
* Correspondence: ssh@kw.ac.kr; Tel.: +82-02-940-5762

Abstract: Underground or submarine cables have a higher capacitance component than overhead lines, and they inject a large amount of capacitive reactive power into the system. A separate reactive power compensation device is required in order for a wind power plant (WPP) connected to the public network with a cable to meet the reactive power requirements required by the grid code. In this paper, a reactive power control using a variable shunt reactor (VSR) was proposed to satisfy the reactive power requirement required by the grid code for a WPP connected to the grid through a cable. The proposed reactive power control method compensates for the capacitive reactive power of the cable by using a VSR, and it follows the reactive power command through the reactive power control of a WPP. In the section where it is difficult to follow the WPP reactive power command only with the reactive power capacity of a WPP due to cable losses or a cable reactive power compensation error of the VSR, the reactive power control is additionally supported through the hysteresis control of the VSR. The proposed method satisfies the grid codes, and it enables fast and accurate reactive power control. The performance of the proposed method was verified through simulation using MATLAB/Simulink.

Keywords: reactive power control; renewable energy; variable shunt reactor; voltage regulation; coordinated control

check for updates

Citation: Song, S.-H.; Kim, S.-B. Coordinated Reactive Power Control with a Variable Shunt Reactor and an Inverter-Based Wind Power Plant. *Energies* **2022**, *15*, 4739. https://doi.org/10.3390/en15134739

Academic Editor: Konstantin Suslov

Received: 18 May 2022
Accepted: 25 June 2022
Published: 28 June 2022

Publisher's Note: MDPI stays neutral with regard to jurisdictional claims in published maps and institutional affiliations.

Copyright: © 2022 by the authors. Licensee MDPI, Basel, Switzerland. This article is an open access article distributed under the terms and conditions of the Creative Commons Attribution (CC BY) license (https://creativecommons.org/licenses/by/4.0/).

1. Introduction

Renewable power plants, such as solar or wind power, which are continuously increasing, are constructed at locations remote from public networks, and they are connected to public networks through long-distance lines. In the case of large-scale renewable power plants, there are many local residents who oppose the construction of transmission towers, so the cases of underground cables are increasing [1–4].

In addition, for offshore wind power plants (WPPs), it is essential to use HV submarine cables for large-capacity, long-distance power transmission. This HV cable has a problem: the construction cost is higher than the overhead line, and the reactive power fluctuation increases due to the large charging current due to capacitance [5].

Charging current exists in all transmission lines and cables due to the inherent capacitive reactance of the conductors [6]. Capacitive reactive power caused by the charging current of transmission lines or cables raises the voltage of the network system, and the higher the voltage level, the greater the charging current that is generated. The shunt capacitance of a transmission line/cable increases as the permittivity of dielectric around the conductor increases; and, since the permittivity of dielectric of the ground is higher than that of air, the charging current is greater in the underground line than in the overhead line [5].

This capacitive reactive power raises the voltage of the system, and as the length of the cable increases, the voltage rise of the charging current increases. Therefore, there are increasing cases where an inductive reactive power compensator needs to be additionally installed to satisfy the grid code at the Point of Connection (PoC).

In the system, it is important to supply inductive reactive power according to voltage rise in light loads and to supply capacitive reactive power according to voltage drop in heavy loads. Grid codes generally require both capacitive and inductive ranges of reactive power that can be supplied according to the amount of active power supplied, and variable control of reactive power according to the command value is required.

Existing reactive power compensation devices include passive compensation devices, such as fixed shunt reactors and variable shunt reactors (VSR) and power electronic device-based compensation devices such as static var compensation (SVC) and static synchronous compensator (STATCOM).

Fixed shunt reactors are typically used to lower grid voltage during light load conditions. In some applications, there is a need to absorb the inductive reactive power in steps, many circuit breakers and foot prints are required in a substation because they consist of multiple shunt reactors and must be frequently connected and disconnected. On the other hand, a VSR is a reactor that can change inductance step by step. The adjustable range of a VSR can be adjusted from the rated reactive power to half the capacity. Moreover, the speed of adjustment is determined by the operation time of the applied tap-changer, which is generally approximately several seconds [7,8].

For applications requiring fast reactive power compensation, SVC or STATCOMs are used. For example, in the event of a grid fault, immediate compensation of reactive power is required to maintain the voltage stability of the power system. In order to control reactive power continuously and dynamically, SVC or STATCOM adjusts reactive power very quickly and continuously through power electronic devices [7,8]. However, FACTS systems such as SVC and STATCOM are more expensive than passive compensation devices.

In case of a wind power plant which is connected by a long cable and its active power output continuously fluctuates, an appropriately designed VSR can be used to follow the reactive power references given by the transmission system operator at the point of connection (POC). However, the number of tap change switches of the VSR increases because the reactive power loss of the cable changes continuously according to the change of the active power, which can affect the lifetime and the reliability of the device. Furthermore, the accuracy of the reactive power control is limited because the VSR output is only discrete depending on the tap position, even though the reactive power command is continuous.

Meanwhile, by use of the inverter-based reactive power control function of individual WTs—which is a key component of the WPP—the reactive power control can be performed according to the reactive power references at the POC. However, it is necessary to accurately determine the reactive power command of each inverter by considering the reactive power loss occurring in the cable between WT and POC. Additionally, the capacity of the inverter should be much larger to compensate for all the losses. Therefore, in case of a long-distance, offshore wind power plant where the capacitive reactive power loss is large, a separate inductive compensation device is absolutely necessary. Maybe a STATCOM is also a possible solution for reactive power control at the POC, but this is very expensive, especially when the size of an offshore WPP is getting bigger and bigger. Therefore, it is necessary to develop a method to effectively integrate and use the reactive power control functions of the VSR and the existing WT.

In this paper, an integrated reactive power control method with a WPP and a VSR is proposed. The proposed reactive power control method compensates for the capacitive reactive power of the cable with the VSR and controls reactive power by wind power according to the reactive power command. The error between the PoC reactive power and the reactive power command caused by the capacitive reactive power compensation error of the VSR and the reactive power loss generated during power exchange is designed to be offset by supplying additional reactive power to the VSR. The proposed method can not only supply reactive power by following the reactive power command quickly and accurately through reactive power control of wind power generators but also satisfy the reactive power supply capacity required by the grid codes at the PoC.

2. Components of Reactive Power Control

2.1. Reactive Power Capability Requirement in Grid Code

In the power system, a large synchronous generator provides a wide range of reactive power capabilities to stabilize the grid voltage. However, as the proportion of existing synchronous generators decreases as the proportion of renewable power in the power system increases, it is necessary to replace the reactive power capacity provided by the existing synchronous generators. Accordingly, most of the grid codes require the capacity to supply reactive power with a leading and lagging power factor of 0.95, even at the rated active power output. Accordingly, the WPP must be designed to meet the reactive power requirements at the point of connection (PoC). Figure 1 shows the requirements for reactive power supply capability proposed in grid codes [9–12]. Within the range of reactive power supply capability shown in Figure 1, the WPP must be able to output reactive power for any reactive power command. In Korea, the grid code was revised in July 2020, and the revised grid codes require a reactive power supply capability of 33% of the rated active power (power factor 0.95 at the rated output) when the active power output is more than 20%.

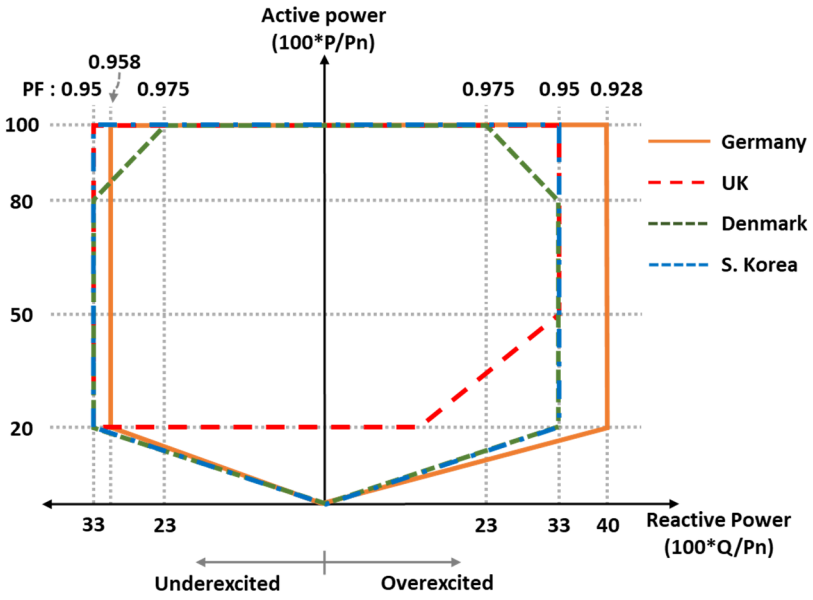


Figure 1. Reactive power capability requirements in various grid codes [7–10].

2.2. Wind Power Plant with High-Voltage Cable and Variable Shunt Reactor

Figure 2 shows the composition of a WPP connected to a transmission line/cable. The WPP can be installed at a long distance from the transmission network operated by a transmission system operator (TSO) for reasons such as environmental conditions and security of site. A WPP connected to the grid through long-distance transmission lines can be installed at a collecting point where a substation for voltage boosting and a line connecting the wind turbines gather. The inverter-based regenerative generator can supply reactive power to the grid within the rated current, and is designed in consideration of the reactive power capacity to satisfy the grid code. However, when the capacity of the wind power generators alone does not satisfy the reactive power supply capacity of Figure 1 at the PoC where the WPP is connected to the grid due to the reactive power losses and charging current of the long-distance transmission line/cable, the reactive power compensation device may be connected separately to the WPP.

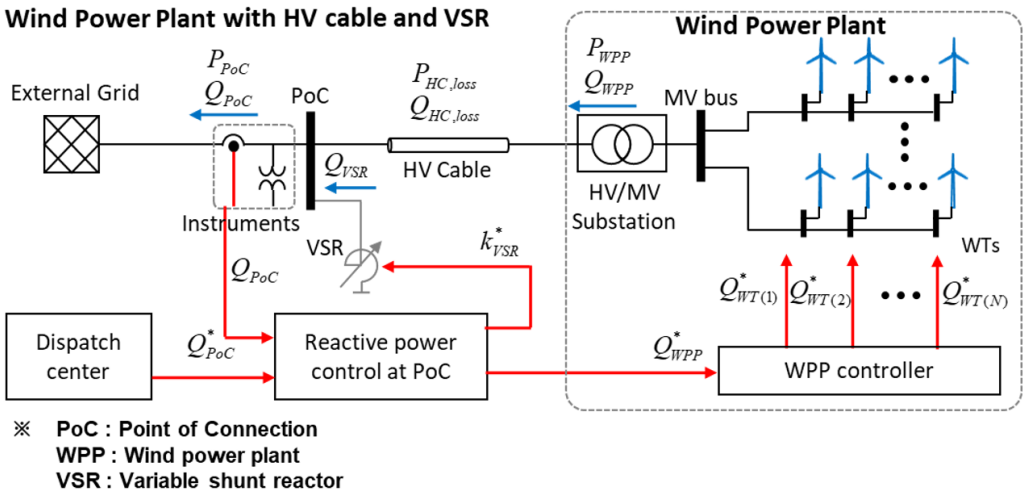


Figure 2. Configuration and reactive power control of wind power plant with HV cable and VSR.

2.3. Effects of High Voltage Transmission Cable

Figure 3 shows the π-type equivalent model of a transmission line/cable and the variation of the reactive power of the WPP at the PoC according to the line/cable impedance. In Figure 4a, voltage difference occurs due to line impedance Z_{TL} $(R_{TL} + jX_{TL})$ while exchanging power between sending bus and receiving bus. If the sending bus in Figure 4a is called PoC in Figure 2 and the receiving bus is the MV bus in the WPP, the PoC voltage can rise by the active power output of wind power generators. And when the line/cable is energized by the parallel susceptance component B_{TL} of the line/cable, capacitive reactive power is injected into the PoC due to the charging current. In the π-type equivalent model of Figure 4a, the series impedance component and the parallel susceptance component increase in almost proportion to the length of the cable.

Assuming that two parallel conductors of radius r and distance d are energized by a voltage source, the potential difference and capacitance between the two conductors are as shown in Equations (1) and (2) [5].

$$V = \frac{q}{\pi\varepsilon} \ln \frac{d}{r} \tag{1}$$

$$C = \frac{q}{V} = \frac{\pi\varepsilon}{\ln \frac{d}{r}} \tag{2}$$

where, ε is the permittivity of the dielectric between conductors. For the overhead line, the permittivity of air is approximately equal to the dielectric constant ε_0 (=8.854 × 10^{-12}) of a vacuum. For a cable, the permittivity of the dielectric around the conductors is generally 2 to 4 times the dielectric constant ε_0 [5].

When a transmission line is installed in the ground or under the sea for a long distance, a large amount of capacitive reactive power is injected into the network system by a very large charging current, which can cause a large increase in the voltage of the transmission network.

If the reactive power capacity of the wind power generator is insufficient due to the series impedance and parallel susceptance of such a transmission line/cable, the reactive power capacity at the PoC can appear as shown in Figure 4b.

In order to provide reactive power to compensate for the capacitive reactive power caused by the charging current of a long-distance underground or submarine cable only by wind power generators, the current capacity of the wind power generators must be increased, which can have a significant impact on the design and cost of the wind power generator have. Therefore, a separate reactive power compensation device is sometimes installed to satisfy the requirement of reactive power supply capability at the PoC of the WPP. In this paper, a VSR is applied as a reactive power compensation device.

2.4. Reactive Power Control with Wind Power Plant

WPP are mainly composed of wind turbines, power-collection systems, and substations, and long-distance high-voltage transmission cables are required when the WPP is constructed far from the public network [13].

The WPP controls reactive power according to the reactive power command of the dispatch center as shown in Figure 3. The reactive power reference generated through the WPP controller is allocated to the wind turbines constituting the WPP. Methods of allocating reactive power references to wind turbines include a method of allocating equally to each turbine, and a method of allocating through optimization considering the internal network and transformer losses, layout of the WPP, and turbine location [14–17].

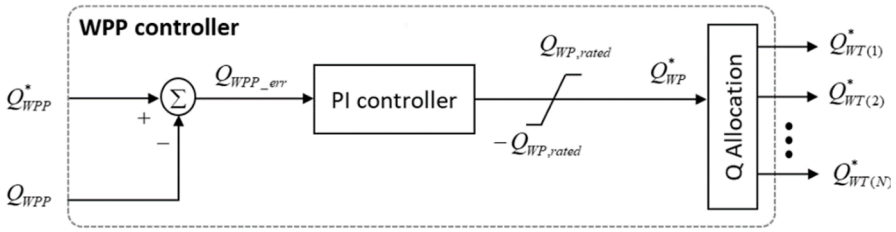


Figure 3. Block diagram for reactive power control of wind power plant [16,17].

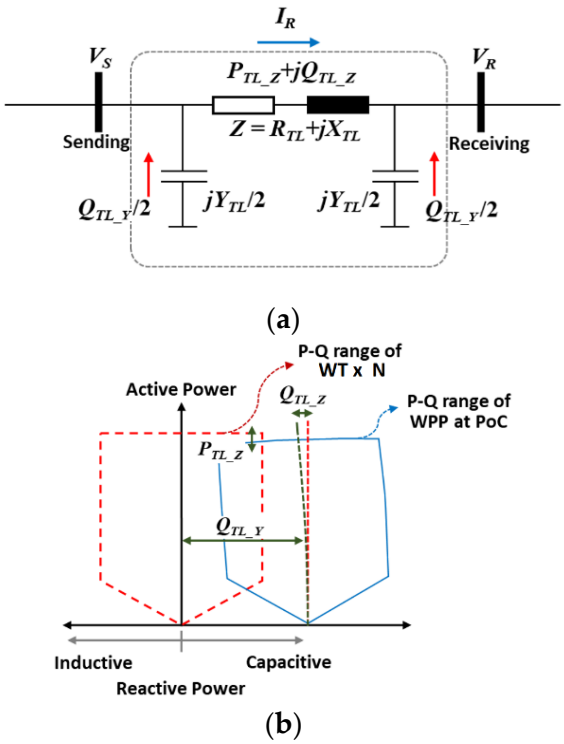


Figure 4. Effects of power transmission cable; (**a**) Equivalent π Circuit for a long transmission line and (**b**) WPP power capability curve at the PoC considering power losses due to the impedance of the transmission line.

If the WPP is installed close to the public network and the reactive power losses of the line/cable connecting the WPP and the public network is negligible, the reactive power capacity of the wind turbines can sufficiently satisfy the reactive power capacity requirement of the grid codes. However, if a WPP is connected to a public network through a long-distance line, the reactive power capacity of the wind turbines must be increased or a separate reactive power compensation device must be installed according to the losses and charging current of the line/cable.

2.5. Reactive Power Control with Variable Shunt Reactor

A VSR is a reactor that can change inductance step by step. The adjustable range of a VSR can be adjusted from the rated reactive power to half the capacity. And the speed of adjustment is determined by the operating time of the applied tap-changer and is generally about several seconds.

The main function of a VSR is to regulate reactive power consumption. This is done by connecting/disconnecting the electrical turns of the reactor. According to Equations (3) and (4), the reactive power consumption of a VSR (Q_{IR}) is proportional to the square of the voltage and inversely proportional to the equivalent inductance (L_R) of the reactor. Considering a constant voltage level, the more inductance, the less current flowing through the VSR branch and less reactive power consumption [7].

$$Q_{IR} \approx \frac{V^2}{L_R} \tag{3}$$

$$L_R \approx \frac{\mu N^2 A}{l} \tag{4}$$

where, μ is the permeability of the core material, l is the physical length of the coil induction component, A is the coil cross-sectional area, and N is the number of electrical turns.

In Equation (4), the inductance of the reactor is proportional to the square of the number of electrical turns.

The reactive power of a VSR is controlled by adjusting the number of electric turns. At the maximum reactive power rating, it is connected by the minimum number of electrical turns and at the minimum reactive power rating, it is connected by the maximum number of electrical turns. Therefore, the minimum reactive power rating is limited by the physical length of the regulating winding and the size of the VSR. This change of number of turns is performed using a tap changer. The same type of tap changer that has been used for decades already in power transformer applications has been used in VSR. Therefore, a VSR can be used to fine tune the power system voltage level [7].

Figure 5 shows the linearly regulated winding arrangement of a VSR.

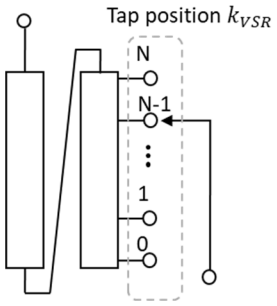


Figure 5. Winding arrangement of a VSR [5].

The reactance size can be adjusted sequentially and the reactive power is discontinuously adjusted due to VSR controls reactive power by adjusting the reactance size through tap switching. In addition, in adjusting the tap, it should be switched at a certain interval, and the tap adjustment time interval is generally about several seconds to several tens of seconds.

3. Reactive Power Control Strategies

3.1. Reactive Power Control at PoC Using Only VSR

The method of adjusting reactive power using a VSR is to sequentially adjust the tap position until the error between the reactive power command and the reactive power of the VSR converges within the tolerance Q_{tol}. Assuming that the PoC reactive power controller in Figure 2 controls the reactive power of the PoC using only a VSR, the reactive power controller of the VSR can be modeled as shown in Figure 6. In Figure 6, if Q_{PoC_err}

is larger than this tolerance Q_{tol}, it outputs a step-up signal, and if Q_{PoC_err} is less than this tolerance Q_{tol}, it outputs a step-down signal. When adjusting the tap, adjust the tap position sequentially at regular intervals.

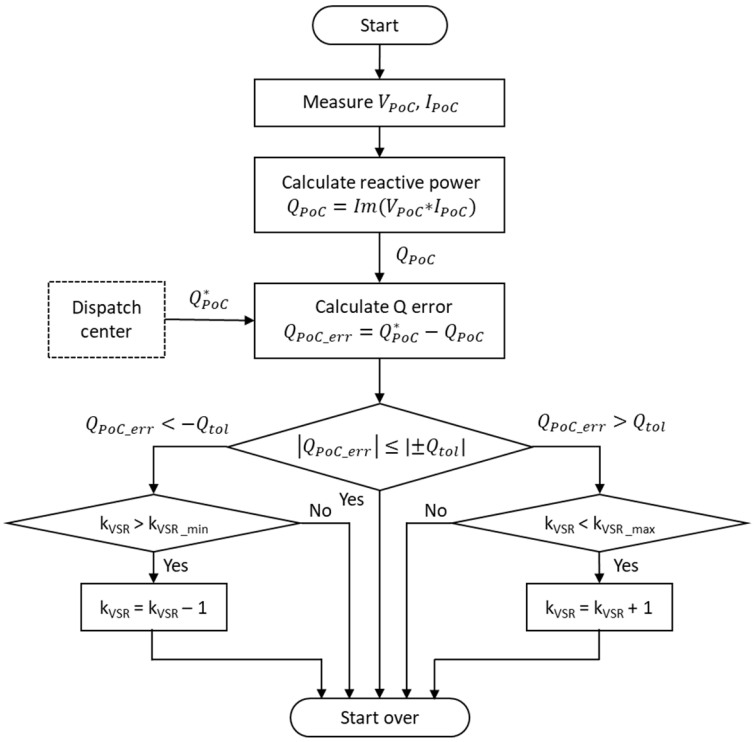


Figure 6. Block diagram of reactive power control of a VSR.

In order to check the operation characteristics of VSR reactive power control, a simulation of reactive power control of the VSR was performed by setting parameters as shown in Table 1 in the WPP model. Figure 7 is the waveform of the VSR reactive power control result when 51.6 [MVar] of reactive power is injected into the PoC by the HV cable as shown in Table 2 in the simulation. In the section where the PoC reactive power command is 0, an error of about 1.8 [MVar] occurred, and in the section where the PoC reactive power command is the reactive power rating of the WPP (26.3 [MVar]), an error of about 1.3 [MVar] occurred. The steady state error of the VSR reactive power control is determined by the amount of reactive power per tap of the adjusted reactive power of the VSR. The smaller the amount of reactive power per tap of the reactive power, the smaller the allowable error range of the reactive power can be set, so the error of the reactive power can be reduced in a normal state. However, it takes a long time for the actual reactive power to reach the reactive power command due to the tap adjustment time delay.

Table 1. Parameters of test VSR model.

Parameters	Unit	Values
Rated active power of wind power plant	MW	80
Rated reactive power of wind power plant	MVar	26.3
Resistance of HV cable	Ω	0.7110
Reactance of HV cable	Ω	1.1985
Admittance of HV cable	Ω^{-1}	0.0015
Maximum rated reactive power	MVar	60
Minimum rated reactive power	MVar	20
Rated voltage	kV	154
Regulating reactive power	MVar	4
time delay	s	1

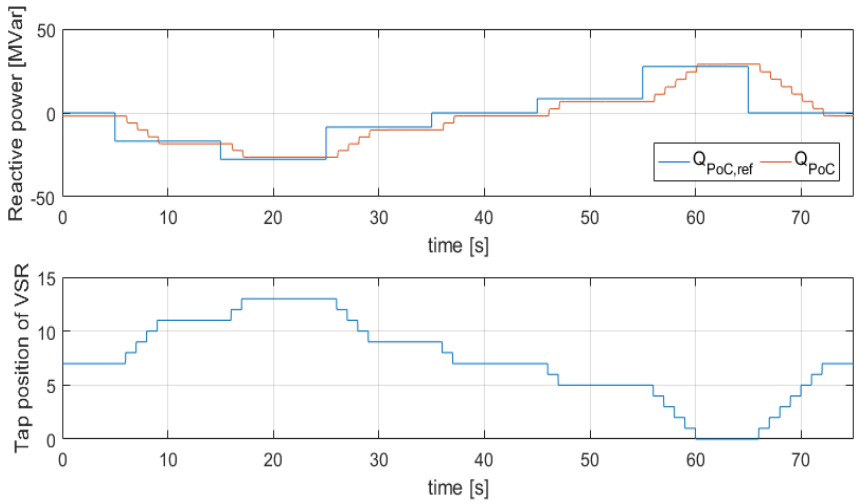


Figure 7. Set–point change of reactive power control using a VSR.

Table 2. Simulation model parameters.

Model	Parameters	Unit	Values
Grid	Nominal power	MVA	100
	Nominal voltage	kV	154
	Nominal frequency	Hz	60
	Swing bus Voltage	kV	156
WPP	Rated power	MVA	84.21
	Rated active power	MW	80
	Rated power factor	-	0.95
	Primary voltage of transformer	kV	154
	Secondary voltage of transformer	kV	22.9
	length of underground cable	km	15
	Resistance of underground cable	Ω	0.7110
	Reactance of underground cable	Ω	1.1985
	Admittance of underground cable	Ω^{-1}	0.0015
VSR	Maximum rated reactive power	MVar	60
	Minimum rated reactive power	MVar	20
	Rated voltage	kV	154
	Number of tap change positions	-	15

In the case of controlling PoC reactive power using only a VSR, it is difficult to precisely control PoC reactive power because the VSR is controlled discontinuously, and it is disadvantageous for maintenance because taps must be changed frequently according to the PoC reactive power command. In addition, when the tap position is fixed according to the line capacitive susceptance and the PoC reactive power is controlled through the reactive power control of the WPP, the error between the reactive power of the VSR and the line capacitive reactive power and the line impedance. Due to the loss of reactive power, it may be difficult to provide the rated PoC reactive power with the reactive power capacity of the WPP.

3.2. Proposed Reactive Power Control Method at the PoC Using WPP and VSR

Reactive power control using only a VSR is discontinuous, and the speed of regulating reactive power is slow because taps must be switched sequentially. On the other hand, an invertor-based wind power generator can control reactive power continuously and accurately with fast response time. In this paper an integrated reactive power control method using a VSR and inverter-based wind power generators is proposed. The proposed method includes a VSR tap change control algorithm and a reactive power feedback

controller for the WPP which is composed of N number inverter-based wind turbines. The use of a VSR is mainly for the compensation of charging current caused by HV cables. However, more or less inductive power from the VSR is desirable if the reactive power command from TSO is not zero at the PoC. The remaining portion of reactive power, which is the difference between the reactive power reference and the actual VSR reactive power, can be supplied by an inverter-based WPP that has proportional feedback and an integral controller, which gives a response that is continuous, accurate, and fast.

Figure 8 shows the block diagram of the proposed reactive power control method. Where K_P, K_I, K_A are the proportional, integral, and anti-windup gain of the controller for the PoC reactive power adjustment, Q^*_{WPP} is the reactive power command of the WPP, k_{VSR_init} is the initial tap position of the VSR to compensate for the charging current of the cable, and k^*_{VSR} is the tap position command of the VSR.

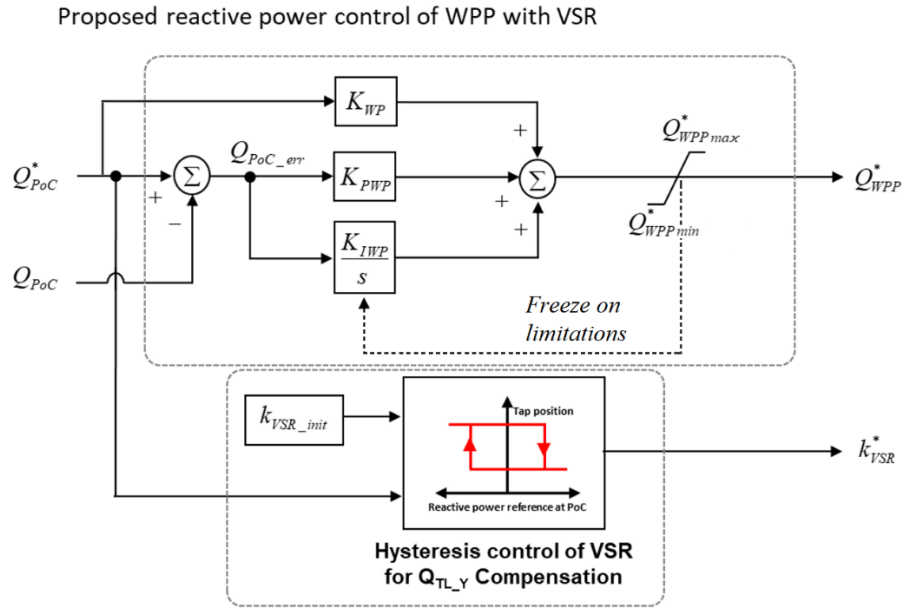
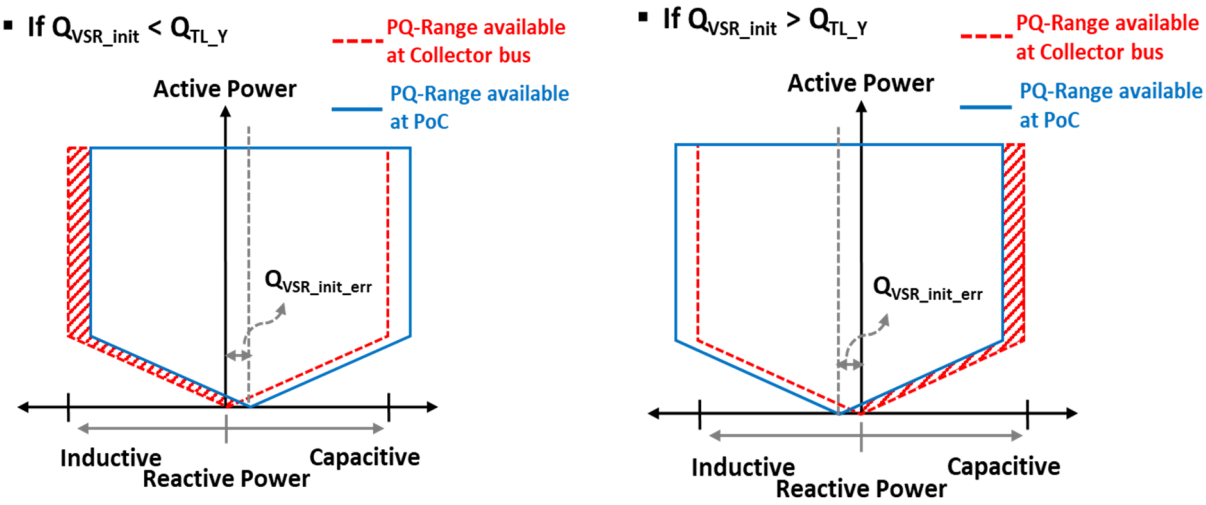


Figure 8. Block diagram of proposed reactive power control of a WPP with a VSR.

In Figure 8, the controller for regulating the PoC reactive power adjusts the reactive power command of the WPP so that the reactive power error at the PoC converges to zero. When the reactive power set-point changes from one value to another, the error is compensated by WPP reactive power control in priority, because the frequent tap change operation of the VSR is not desirable due to maintenance and life time issues. However, when the required amount of reactive power is larger than the capacity of the WPP reactive power rating, the hysteresis controller activates the tap change of the VSR in the proposed method. Using such a sophisticated combination of a VSR and a WPP, the proposed reactive power control method can achieve a large power rating with a VSR and a fast and an accurate response with an inverter-based WPP.

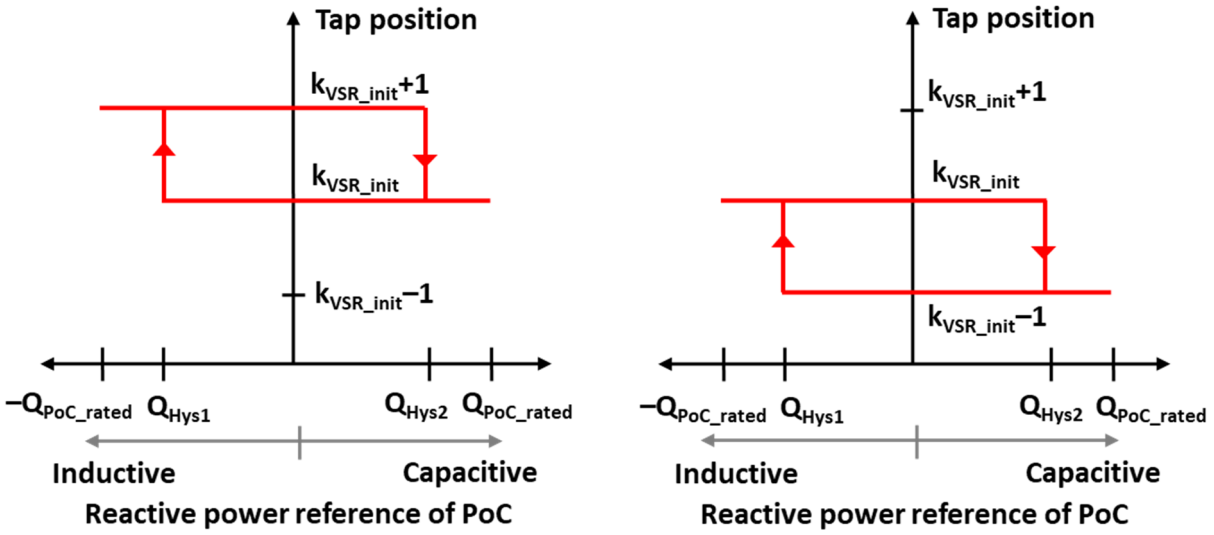
As shown in Figure 4b, the reactive power capability at the PoC is different from that of number N with turbines due to the cable capacitance and inductance. Additionally, the VSR reactive power can have an initial compensation error $Q_{VSR_init_err}$ because the VSR reactive power has only discrete values, whereas the actual cable reactive power is continuous. In Figure 9, the red dotted line is the P-Q range that can be controlled by the WPP at the collecting bus of the WPP, and the blue solid line is the P-Q range that can be controlled by the WPP at the PoC. If the $Q_{VSR_init_err}$ is capacitive, it may not be possible to supply sufficient inductive reactive power in the shaded section, as shown in Figure 9a. In the opposite case, when $Q_{VSR_init_err}$ is inductive, a shaded section where it is difficult to supply capacitive reactive power occurs, as shown in Figure 9a.



(**a**) (**b**)

Figure 9. Hysteresis control concept diagram; (**a**) Hysteresis control setting when cable reactive power compensation error of the VSR is capacitive; (**b**) Hysteresis control setting when cable reactive power compensation error of the VSR is inductive.

The proposed method additionally adjusts the tap of the VSR with hysteresis control according to the PoC reactive power command, as shown in Figure 10, so that sufficient reactive power can be provided even in the shaded section of Figure 9, where Q_{Hys1} and Q_{Hys2} denote the hysteresis band.



(**a**) (**b**)

Figure 10. Hysteresis control concept diagram; (**a**) Hysteresis control setting when cable reactive power compensation error of the VSR is capacitive; (**b**) Hysteresis control setting when cable reactive power compensation error of the VSR is inductive.

If $Q_{VSR_init_err}$ is capacitive, as shown in Figure 9a, tap up the VSR to supplement inductive reactive power when the PoC reactive power command falls below Q_{Hys1}, as shown in Figure 10b. In the opposite case, if $Q_{VSR_init_err}$ is capacitive as shown in Figure 9b, tap down the VSR to reduce inductive reactive power when the PoC reactive power command rises above Q_{Hys2}, as shown in Figure 10b.

Tap switching through hysteresis control can reduce the number of tap switching according to the change of reactive power command of the PoC.

4. Simulation

4.1. Implementation

To simulate the cooperative reactive power control of the WPP and the VSR, the system model and the VSR and the WPP models were implemented using MATLAB/Simulink tools. To simplify the simulation and to shorten the computing time, phasor mode simulation was used for all calculations and modeling. In order to avoid switching effects in the simulation, the VSR model of MATLAB/Simulink was designed with a number of parallel reactors that were merged step by step. In the VSR model, the tap switch below the tap position command was closed when the tap position command was input, and the parallel sum of the reactances where the tap switch was closed became the reactance magnitude of the regulating winding. As the tap position increased, the reactance of the tap switch of the adjustment winding increased so that the total reactance decreased and the reactive power consumed increased.

The WPP model was implemented based on the standard IEC 61400-27 for electrical simulation models of wind power generation. The wind power generation simulation model of IEC 61400-27 is a fundamental wave RMS model that can be used to analyze the stability of large-scale power systems and grids of wind turbines and WPPs, and it was developed to simulate the dynamic characteristics of events of various power systems [18,19].

The WPP model implemented in this paper was composed of a WPP controller and a wind turbine model, and the wind turbine was implemented as a type 4 model, a wind turbine type based on a full-scale converter.

The system model was implemented using the parameters of some transmission network systems in Jeollanam-do, Korea. Approximately 80 MW of wind power generation is connected to the Yeonggwang substation in Jeollanam-do, managed by KEPCO, the TSO of Korea, and the renewable power generation is connected to the Yeongwang substation through an underground line of approximately 15 km. Approximately 50 MVar of capacitive reactive power is injected into the Yeonggwang substation by the charging current of the WPP's underground line. In this paper, the Yeonggwang substation was set up as the PoC, and the VSR was connected to the Yeonggwang substation. Table 2 shows the parameters of the system model, and Figure 11 shows the system model implemented in the simulation.

Through simulation, the PoC reactive power is controlled using only a VSR and the performance of the reactive power control of the proposed method is compared.

In both methods, the conditions for energizing the line and outputting the WPP were the same.

4.2. Simulation Results

Reactive power control using only a VSR and the P-Q curve of the PoC in the steady state of the proposed scheme were compared. Figure 12 shows the P-Q curve of the proposed method and the reactive power control using only a VSR. In the reactive power control using only VSR in Figure 12, when the active power output is 0, there is an offset of approximately 0.03 [pu] in the reactive power. The output was insufficient and exceeded in the capacitive reactive power.

The proposed scheme controlled the PoC reactive power to 0 when the active power output was 0. In addition, the reactive power was controlled to match the inductive and the capacitive reactive power rating even in the range of 0.2 [p.u] or more of the active power output.

Reactive power and the initial operation of the VSR by a charging current at the initial energization of the simulated WPP transmission line were simulated. In the simulation, the WPP transmission line was energized at the simulation time of 1 s, and the tap position adjustment of the VSR for line capacitive reactive power compensation was started at the

simulation time of 5 s. Additionally, the WPP operation was started at 15 s of simulation time. Figure 13 shows the operation waveform during initial energization of the transmission line. In Figure 13, approximately 51.7 MVar of capacitive reactive power was injected into the PoC immediately after the line was energized, and the PoC voltage increased from 157.5 kV to 162.5 kV. As the VSR operated and the VSR sequentially adjusted the tap position, the PoC reactive power decreased to 2.5 MVar and the PoC voltage decreased to 157.8 kV. When the WPP operation started and the WPP output was 0.9 p.u of the WPP rating, the PoC voltage rose to 158.9 kV.

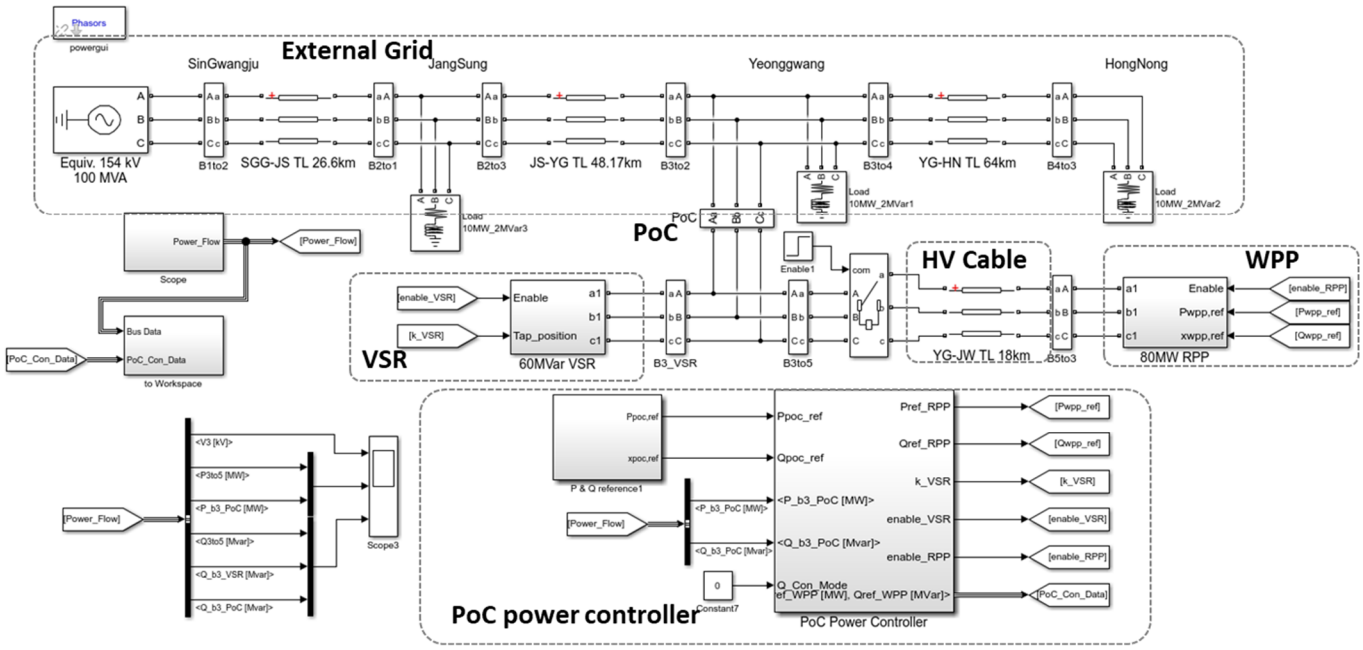


Figure 11. Simulation model of wind power plant with HV cable and VSR using MATLAB/Simulink.

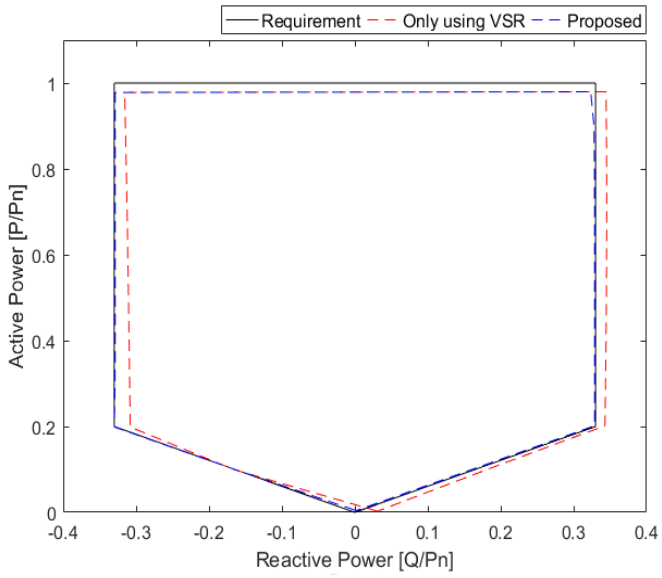


Figure 12. Reactive power capability by reactive power control method.

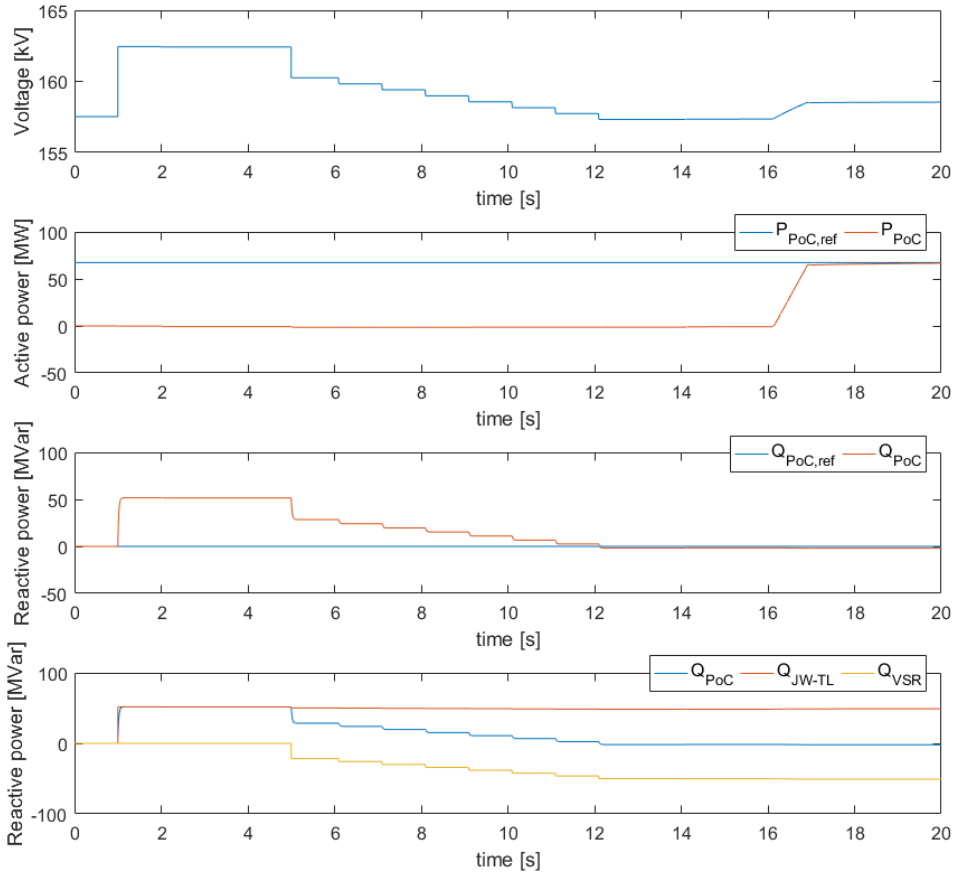


Figure 13. Reactive power capability by the reactive power control method.

Figure 14 is the result of set-point change control when the PoC reactive power control is performed using only a VSR, and Figure 15 is the result of set-point change control waveform when the PoC reactive power control is performed in the proposed method. The top waveforms in Figures 14 and 15 represent the PoC reactive power and the reactive power command for each control method; the second waveform from the top is the PoC reactive power error; the third waveform from the top is the tap position of the VSR; and the last waveform is the PoC voltage for each control method. The deviation between the power commands and the lowermost part indicates the tap position of the VSR.

In the case of reactive power control using only a VSR in Figure 14, there is an error with the reactive power command, and it takes several seconds to converge to the approximate value of the reactive power command by adjusting the tap position sequentially at time intervals. Moreover, according to the change of the reactive power command, the tap position adjustment of the VSR occurs frequently. In the case of the proposed method in Figure 15, there is no reactive power error, and the reactive power command is converged in tens of ms. In addition, the tap position of the VSR is adjusted only in the section where the reactive power command is close to the inductive or capacitive reactive power rating, and there is no tap adjustment in the section below that.

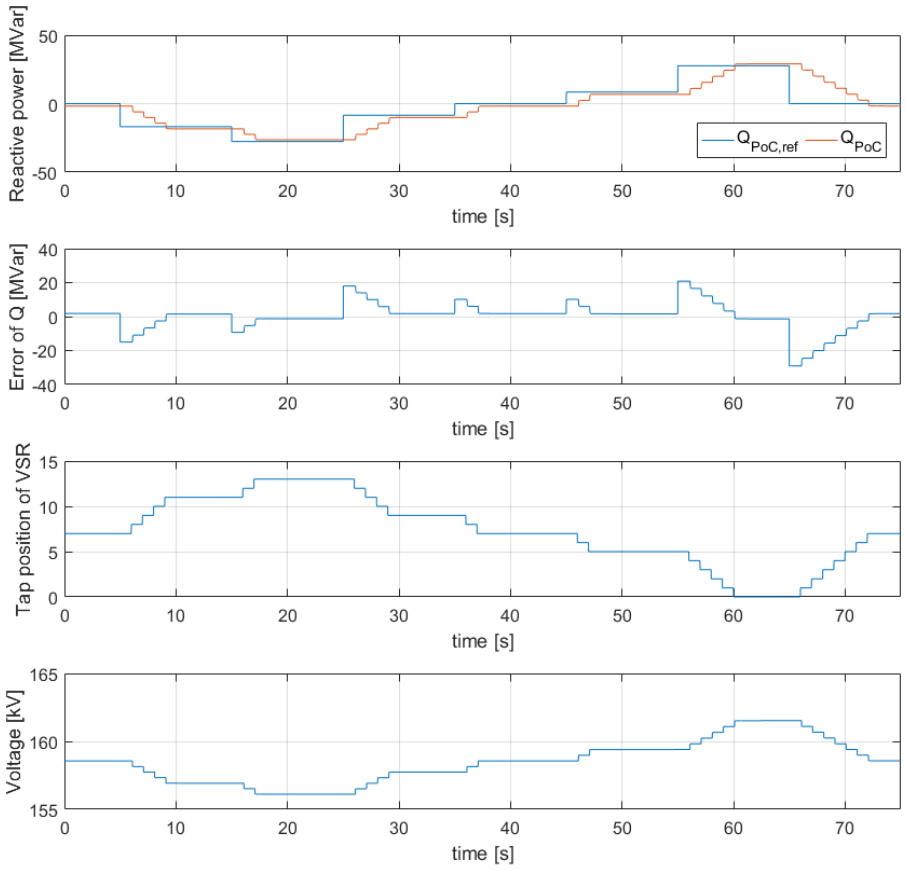


Figure 14. Set–point change control response of reactive power using only a VSR.

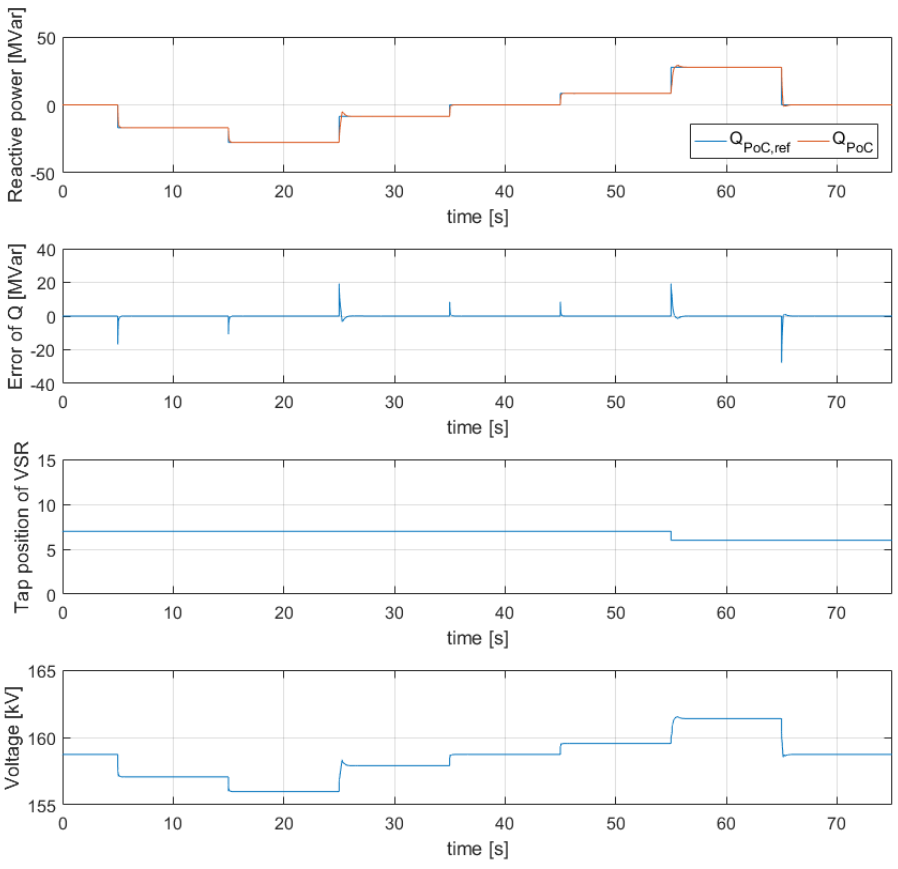


Figure 15. Set–point change control response of reactive power using proposed method.

5. Conclusions

WPPs that are connected to the high-voltage transmission network over long distances through underground or submarine cables have difficult satisfying the reactive power supply capability required by the grid codes at the PoC due to the charging current of the long-distance cables. Accordingly, a separate reactive power compensation device is required. In this paper, we proposed a reactive power control method that can satisfy the requirements of reactive power supply capability at the PoC by applying a VSR to a WPP connected to the grid through a long-distance transmission cable. The VSR controls taps in a non-linear and a physical way through tap switching, so the control speed is also slower than that of power converters. On the other hand, in the case of a WPP, reactive power control is possible at a continuous and a fast speed by controlling the reactive power of wind turbines based on a power converter. The proposed method compensates for the charging current of a long-distance line through the VSR and follows the PoC reactive power command through the reactive power control of the WPP to control the PoC reactive power with fast response characteristics while satisfying the requirements of the grid codes. In the section where the VSR is fixed and it is difficult to output the rated reactive power only with the reactive power capacity of the WPP, the VSR supplies additional reactive power through hysteresis control. In addition, when the WPP reactive power capacity required for PoC reactive power control is insufficient due to the line reactive power losses, the VSR can supplement PoC reactive power through additional tap adjustment, thereby compensating the charging current of the VSR. Reactive power supply capability can be satisfied at the PoC even for reactive power losses of the cable. The performance of the proposed method was analyzed through simulation, and as a result of the simulation, the proposed method showed no error in steady state and showed a very fast response speed compared to the reactive power control using only a VSR.

Author Contributions: All authors contributed to publishing this paper. S.-B.K. and S.-H.S. mainly proposed the algorithm of this paper. S.-B.K. carried out the simulation tests, and he revised the original scheme. Writing was done by S.-B.K. and S.-H.S. Final review was done by all authors. All authors have read and agreed to the published version of the manuscript.

Funding: This work was initiated and conducted during the sabbatical year of Kwangwoon University in 2012 and this work was also supported by the Korea Institute of Energy Technology Evaluation and Planning (KETEP) and the Ministry of Trade, Industry & Energy(MOTIE) of the Republic of Korea (No. 20193710100061).

Institutional Review Board Statement: Not applicable.

Informed Consent Statement: Not applicable.

Data Availability Statement: Not applicable.

Conflicts of Interest: The authors declare no conflict of interest.

References

1. Tziouvaras, D.A.; Needs, J. Protection of mixed overhead and underground cable lines. In Proceedings of the 12th IET International Conference on Developments in Power System Protection (DPSP 2014), Copenhagen, Denmark, 31 March–3 April 2014; pp. 1–6.
2. Su, C.Q. Failure analysis of three 230 kV XLPE cables. In Proceedings of the 2010 IEEE/PES Transmission & Distribution Conference & Exposition: Latin America (T&D-LA), Sao Paulo, Brazil, 8–10 November 2010; pp. 22–25.
3. Im, J.; Kang, S.; Song, S.; Jung, S.; Choi, J.; Choy, I. Reactive Power Control Strategy for Inverter-based Distributed Generation System with a Programmable Limit of the Voltage Variation at PCC. In Proceedings of the 8th International Conference on Power Electronics–ECCE Asia (2011), Jeju-do, Korea, 30 May–3 June 2011.
4. Im, J.; Song, S.; Kang, S. Analysis and Compensation of PCC Voltage Variations caused by Wind Turbine Power Fluctuations. *J. Power Electron.* **2013**, *13*, 854–860. [CrossRef]
5. Xue, Y. Charging current in long lines and high-voltage cables-protection application considerations. In Proceedings of the 39th Annual Western Protective Relay Conference, Washington, DC, USA, 15–18 October 2012.
6. Bell, J.; Hargrave, A.; Smelich, G.; Smyth, B. Considerations when using charging current compensation in line current differential applications. In Proceedings of the 72nd Annual Conference for Protective Relay Engineers (2019), College Station, TX, USA, 22–25 March 2019; pp. 1–11.

7. Khorami, M. Application fields and control principles of variable shunt reactors with tap-changer. Master's Thesis, Department of Energy and Environment, Division of Electric Power Engineering, Chalmers University of Technology, Göteborg, Sweden, 2011.
8. Qin, N. Voltage Control in the Future Power Transmission Systems. Ph.D. Thesis, Department of Energy Technology Aalborg University, Aalborg, Denmark, 2016.
9. Tennet TSO GmbH. *Grid Code—High and Extra High Voltage*; Tennet TSO GmbH: Bayreuth, Germany, 2012.
10. NGET. The Grid Code (Issue 5, Revision 46). Available online: https://www.nationalgrideso.com/industry-information/codes/grid-code/code-documents (accessed on 10 December 2020).
11. Energinet.dk. *Technical Regulation 3.2.5 for Wind Power Plants with a Power Output Greater than 11 kW*; Transmission System Operator of Denmark: Fredericia, Denmark, 2010.
12. KEPCO. The Provision for Using Transmission and Distribution Systems. 2020. Available online: http://cyber.kepco.co.kr/ckepco/front/jsp/CY/H/C/CYHCHP00601.jsp (accessed on 10 October 2020).
13. Feng, L.; Ping, Y.; Qunru, Z.; Zhou, S.; Qian, W. Research on reactive power compensation optimization design based on equivalent model of offshore wind farm. In Proceedings of the IEEE Asia-Pacific Power Energy Engineering Conference, Hong Kong, China, 7–10 December 2014; pp. 1–6.
14. Gao, H.C.; Yun, S.Y.; Choi, J.H.; Ahn, S.J. Reactive Power Allocation Method in a Wind Farm for Improved Voltage Profile and Loss Reduction. *Int. J. Eng. Res. Technol.* **2018**, *12*, 2167–2182.
15. Nguyen, T.H.; Lee, D.C.; Van, T.L.; Kang, J.H. Coordinated control of reactive power between STATCOMs and wind farms for PCC voltage regulation. *J. Power Electron.* **2013**, *13*, 909–918. [CrossRef]
16. Rakaram, R.; Kumar, K.S.; Rajasekar, N. Power system reconfiguration in a radial distribution network for reducing losses and to improve voltage profile using modified plant growth simulation algorithm with distributed generation. *Energy Rep.* **2015**, *1*, 116–122. [CrossRef]
17. Mokui, H.T.; Masoum, M.A.; Mohseni, M. Enhanced reactive power allocation of full converter wind generation system. In Proceedings of the IEEE 5th International Symposium on Power Electronics for Distributed Generation System, Galway, Ireland, 24–27 June 2014; pp. 1–6.
18. IEC 61400-27-1:2015. Ed.1: Wind Turbines—Part 27-1:Electrical Simulation Models for Wind Power Generation. IEC: Geneva, Switzerland, 2015.
19. Sorensen, P.; Andresen, B.; Fortmann, J.; Johansen, K.; Pourbeik, P. Overview, status and outline of the new IEC 61400-27 electrical simulation models for wind power generation. In Proceedings of the 10th International Workshop on Large-Scale Integration of Wind Power into Power Systems, Aarhus, Denmark, 25–26 October 2011.